Waypoint Guidance for Small UAVs in Wind

John Osborne* and Rolf Rysdyk†
University of Washington, Seattle, WA, 98115,USA

I. abstract

Wind is often ignored or only implicitly addressed in design of guidance algorithms. For small UAVs exposed to strong winds, wind has a very significant nonlinear effect on the guidance algorithm, and strongly affects the spatial orientation and rates of the vehicle. In this work, an autonomous Unmanned Aerial Vehicle (UAV) is commanded to fly along a path defined by a series of waypoints. The guidance algorithm includes an observer based wind estimator. Based on estimated wind speed and direction, the airspeed and desired course change, a proximity distance is retrieved from a lookup table for each waypoint. This distance allows the aircraft to smoothly converge to each new course, without over/under shoot, in strong wind conditions. This capability is significant in various tactical maneuvers, e.g. surveying, multi-vehicle operations, target observation, target tracking, avoiding detection, etc.

Nomenclature

χ_s	desired aircraft course
χ_n	next aircraft course
$\Delta\chi$	total change in aircraft course during a turn
d_p	waypoint proximity distance
y_s	crosstrack error
$\mathbf{P(t)}$	coordinates of aircraft position
$\mathbf{W}$	complete waypoints list
$\mathbf{W_p}$	coordinates of previous waypoint
$\mathbf{W_c}$	coordinates of current waypoint
$\mathbf{W_n}$	coordinates of next waypoint

II. Introduction

Wind has a very significant nonlinear effect on the guidance algorithms for small UAVs operating in strong winds. The wind strongly affects the inertial orientation and rates of the vehicle. Similar operating conditions apply to some large high altitude UAVs that may be exposed to jet-stream effects. An example is the Boeing Condor UAV which could be guided to 'fly back-wards' in high winds at altitude.[1]

A human pilot learns to estimate the exposure to wind from experience, visual information, and 'seat-of-the-pants' feel. The human pilot predicts its effects and will use appropriate anticipatory guidance commands when changing course or maneuvering. In un-anticipatory waypoint flying, once a waypoint has been achieved, the aircraft begins a turn to the next waypoint. This results in an overshoot of the desired flight path, which can be substantial. For long distance navigation this may be acceptable, but when the waypoint segment lengths are of the order of magnitude of the aircraft turn radius, this overshoot becomes an issue of serious concern.

One remedy for the overshoot is to pre-program a 'look-ahead' distance into the simulation, so that once the aircraft is within a given distance of a waypoint, it begins a turn toward the next waypoint. Intelligent

*Graduate Student, Aeronautics and Astronautics, Student Member AIAA
†Assistant Professor, Aeronautics and Astronautics, rysdyk@aa.washington.edu, Member AIAA

selection of this look-ahead distance can lead to a reduction in overshoot. For precision flight with limited maneuvering space we are interested in turns at maximum bank angle without overshoot. We assume that airspeed is constant, but that the inertial speed varies significantly due to wind. The flightpath design involves similar considerations as e.g. Chandler et al.,[2] who proposed linking adjoining path segments with curvature determined by the minimum turn radius of the vehicle. Kuwata and How[3] used similar ideas for flight path planning in 'urban terrain', i.e. highly restricted maneuvering space. Both of these approaches rely on the minimum turn radius of the aircraft in a zero wind environment. In this perspective, the effect of wind is twofold; it alters the minimum achievable radius by affecting inertial velocity, and the curvature of the flight path is no longer constant.

The presented work is one attempt to ensure maximum performance convergence without overshoot to the desired course, in a variety of wind conditions. The following considerations went into the proposed solution:

- avoid undue heuristical constructs,
- allow for zero or negative groundspeed,
- allow for multi-vehicle coordination,
- minimize reliance on high bandwidth computation and communication, and
- allow easy integration with path planning and path generation algorithms.

The first two items provide necessary robustness. The third and fourth considerations preclude elegant iterative solutions as e.g. in [4]. The last consideration typically involves a translation from crude data to smooth and/or feasible paths. Furthermore, this data is often in the form of simple waypoints, i.e. {latitude,longitude} sets of a sequence of locations. In this work we are specifically concerned with the "Evolution based Cooperative Planning System",[5] which generates paths consisting either of a list of waypoints or a sequence of lines and constant curvature arcs.

The solution proposed here is a lookup table which selects an appropriate 'look-ahead' distance, in response to a desired course change, wind heading, wind speed, and airspeed. When the distance between the aircraft and the current waypoint is less than this 'proximity distance', the aircraft rolls to maximum bank angle to begin turning towards the next waypoint.

For initial evaluation, a Matlab Simulink model is built consisting of navigation, guidance, and control loops about a dynamic model of a small UAV with atmospheric dynamics.[6] The innerloops consist of straightforward stability augmentation for airspeed and altitude, and allow for a bank angle command tracking. The bank angle command is generated by a guidance loop, 'helmsman',[7] based on cross-track error feedback. The desired ground-track is generated by a navigation module, which follows a series of arbitrary waypoints, automatically recalling the appropriate proximity distance from the lookup table. Results are demonstrated for several representative flight paths.

III. The Effects of Wind

A maximum bank angle turn, conducted without wind, results in a ground track that is a smooth, clean circle, as seen in Figure III. Under these conditions, the minimum turn radius is clearly defined as a function of airspeed. The same maximum bank angle turn over the same flight time produces dramatically different results in the presence of wind. Figure III shows that the notion of a 'minimum turn radius' does not apply in a windy environment.

In this work we assume that the UAV will fly *inertially coordinated* turns. A 'coordinated turn' is one in which the resultant of gravity and centrifugal force lies in the aircraft plane of symmetry.[8] For an inertially coordinated turn, the associated kinematics can be approximated as

$$\dot{\chi} = \frac{g}{V_g} \tan\phi \tag{1}$$

(assuming that $V_g > 0$). The inertial position of the aircraft can be expressed in terms of the inertial course and ground speed:

$$\dot{x}_N = V_g \cos\chi \tag{2}$$
$$\dot{y}_E = V_g \sin\chi \tag{3}$$

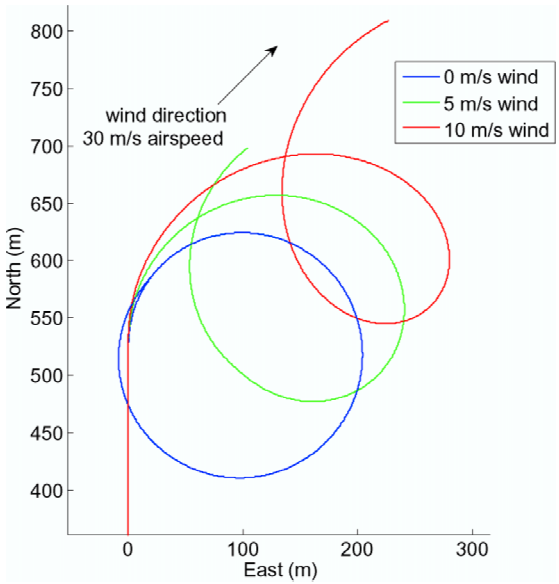

Figure 1. Open loop flight simulation. Wind is 0, 5, and 10 m/s from 225°.

The effect of wind is included as

$$V_a \cos(\psi) = V_g \cos(\chi) + V_w \cos(\psi_w) \tag{4}$$

$$V_a \sin(\psi) = V_g \sin(\chi) + V_w \sin(\psi_w) \tag{5}$$

Wind affects the relation between course and heading. The heading is obtained from the above as:

$$\psi = \text{atan2}\left\{\frac{V_g \sin\chi + V_w \sin\psi_w}{V_g \cos\chi + V_w \cos\psi_w}\right\} \tag{6}$$

where atan2 represents the 4-quadrant tangent function. In strong winds, a distinction must be made between the inertial course rate-of-change and the heading rate-of-change. This is not commonly addressed in the literature. Neglecting the effect of bank-angle dynamics and considering kinematics only, the effect of wind on the course-rate-of-change as compared with yaw-rate can be seen by manipulation of expressions (4) and (5) to obtain:

$$V_g^2 = V_a^2 + V_w^2 - 2V_a V_w \cos(\psi - \psi_w) \tag{7}$$

$$\tan\chi = \frac{V_a \sin\psi - V_w \sin\psi_w}{V_a \cos\psi - V_w \cos\psi_w} \tag{8}$$

Consider that V_w, and ψ_w are constant, and V_a varies slowly. We can find from Eqn(8) that:

$$\frac{\dot{\chi}}{\dot{\psi}} = \frac{\cos^2\chi}{(\cos\psi - V_w/V_a \cos\psi_w)^2}\left\{1 - \left(\frac{V_w}{V_a}\right)\cos(\psi - \psi_w)\right\} \tag{9}$$

Combining this expression with Eqn (8) indicates how the yaw-rate compares to the course-rate-of-change in various orientations and for various wind speeds. The result is shown in figure 2, which shows that the course-rate-of-change can be dramatically different from the yaw-rate in strong winds.

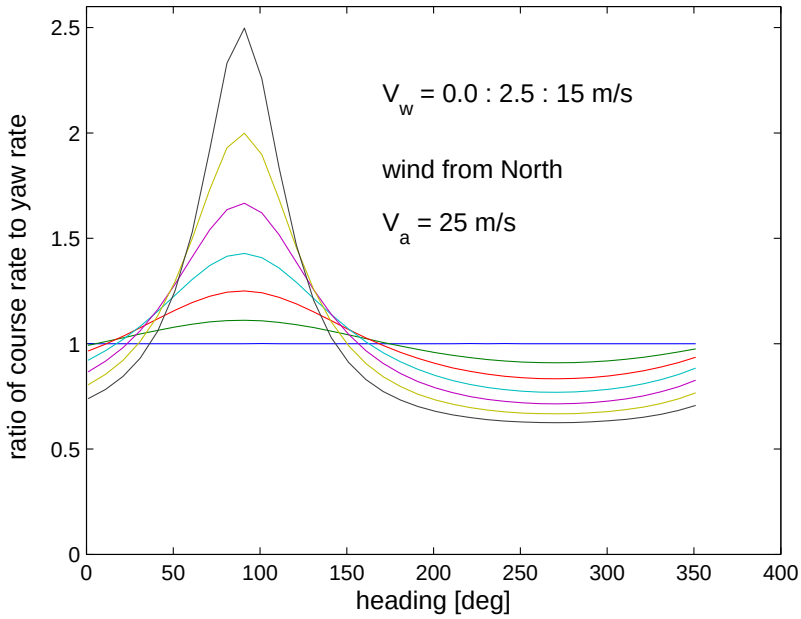

Figure 2. Course-rate-of-change to yaw-rate ratio in various wind speeds while vehicle has an airspeed of $25\ m/s$**.**

IV. Waypoint Flying

The first aspect of this project involved the navigation module to allow the aircraft to follow a series of waypoints. A waypoint list is built as

$$\mathbf{W} = \begin{bmatrix} w_{1_x} & w_{1_y} & w_{1_z} \\ w_{2_x} & w_{2_y} & w_{2_z} \\ \vdots & \vdots & \vdots \\ w_{m_x} & w_{m_y} & w_{m_z} \end{bmatrix} \tag{10}$$

This waypoint list is input to the Simulink model, and the current course χ_s is calculated as

$$\chi_s = \arctan\left(\frac{\mathbf{W_{c_y}} - \mathbf{W_{p_y}}}{\mathbf{W_{c_x}} - \mathbf{W_{p_x}}}\right) \tag{11}$$

and the next course χ_n is calculated as

$$\chi_n = \arctan\left(\frac{\mathbf{W_{n_y}} - \mathbf{W_{c_y}}}{\mathbf{W_{n_x}} - \mathbf{W_{c_x}}}\right) \tag{12}$$

based on the current waypoint $\mathbf{W_c}$, the previous waypoint $\mathbf{W_p}$, and the next waypoint $\mathbf{W_n}$ extracted from the waypoint list.

For the UAV under consideration, a path following helmsman is in place,[7] which converges with the desired path by means of a 'helmsman' strategy (Figure 4) and keeps track of its progress along the desired path by means of a Serret-Frenet projection.[9,10] In the current work the aircraft is constrained to a constant altitude. Additionally, the flight segments are straight, which simplifies the computations. Figure 3 illustrates the definition of variables used for the general two dimensional Serret-Frenet reference frame. For our work, the variable of interest is y_s, the aircraft's cross-track error. For flight along a curved spline, the Serret-Frenet

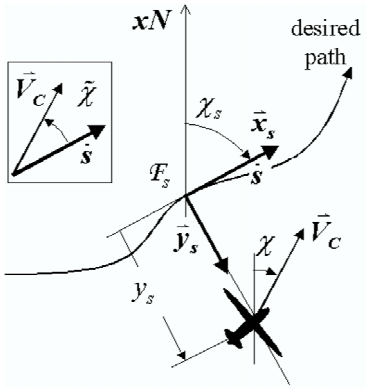

Figure 3. The Serret-Frenet reference frame for a 2-D path.

transformations are

$$\begin{pmatrix} \dot{s} \\ \dot{y}_s \\ \dot{\tilde{\chi}} \end{pmatrix} = \begin{pmatrix} \frac{V_g \cos(\tilde{\chi})}{1-\kappa y_s} \\ V_g \sin(\tilde{\chi}) \\ \dot{\chi} - \frac{V_g \cos(\tilde{\chi})\kappa}{1-\kappa y_s} \end{pmatrix} \tag{13}$$

Because in waypoint flying the commanded flight paths are restricted to linear segments ($\kappa = 0$), these reduce to

$$\begin{pmatrix} \dot{s} \\ \dot{y}_s \\ \dot{\tilde{\chi}} \end{pmatrix} = \begin{pmatrix} V_g \cos(\tilde{\chi}) \\ V_g \sin(\tilde{\chi}) \\ \dot{\chi} \end{pmatrix} \tag{14}$$

The aircraft's distance from its desired course is computed as

$$y_s = \int_0^t \dot{y}_s \, \mathrm{d}t + y_0 \tag{15}$$

where y_0 is the initial distance from the desired course. For pure waypoint flying, $y_0 = 0$; waypoint switching occurs as the aircraft passes through $\mathbf{W_c}$. y_s determines the commanded course $\tilde{\chi}_c$, as shown in Figure 4.

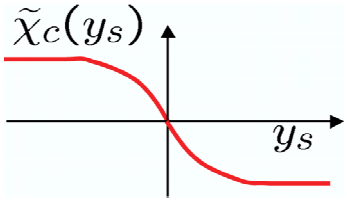

Figure 4. The behavior of a 'good helmsman'. $\tilde{\chi}_c$ is the commanded intercept angle, y_s is the cross-track error.

V. Lookup Table

The aim of the lookup table is to ensure maximum performance course convergence without overshoot, in a variety of wind conditions. Although it may be possible to use an analytic expression based on kinematic approximations alone, the lookup table generation also allows also for: inclusion of dynamic effects which may be significant for large aircraft or in case of low bandwidth command tracking; communication and computational delays; nonlinear performance and actuation limits; non-positive ground speed; and other considerations like e.g. radar signature concerns.

The input to the lookup table, which are assumed constant during the maneuver for course change, will include: initial course, desired course change, wind speed and direction, and vehicle airspeed. In this work, the output is limited to the required 'look ahead' or 'proximity' distance necessary to allow for the maximum

performance course change. This distance is used to initiate the turn to the new course. An example is indicated in Figure 5.

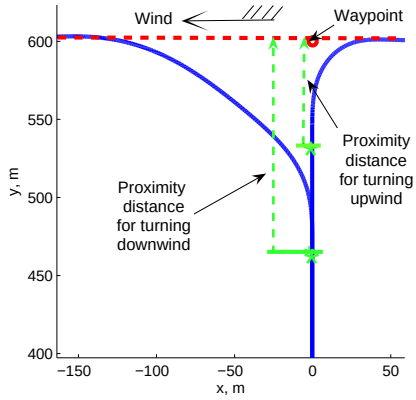

Figure 5. Examples of proximity distance generation. Starting from a crosswind course, changing course downwind requires a larger proximity distance than an upwind course change.

For further integration with path planning and path generation tools, the output can also include e.g. time and location of convergence, which can be used for coordination of multiple vehicles.

A Simulink model of the Aerosonde UAV[6] is used for the lookup table construction and for the examples that follow. This is a full 6 D.O.F. nonlinear model which was used unmodified with exclusion of the turbulence model. The aircraft includes actuation dynamics and limits. Simple PID feedback was used to stabilize the aircraft and allow for a bank angle command.

To construct the lookup table, the aircraft is commanded to make a 175° turn starting from a known location, and its position and course are recorded at every time step. As in the actual flight model, a coordinated turn is made at the maximum allowable bank angle. At the increments shown in Table 1 for $\Delta\chi$, a tangent line is calculated from the aircraft's position to the x axis. The difference between this x axis intercept point and the point where the turn command is given is the appropriate proximity distance for the given turn.

Table 1. Lookup Table Inputs

Parameter	Min.	Incr.	Max.
Course Change	0°	5°	175°
Wind Direction	0°	30°	360°
Wind Speed	0 m/s	2 m/s	18 m/s
Commanded Airspeed	20 m/s	5 m/s	35 m/s

The simulation code is executed for each relative wind heading, wind speed, and airspeed listed in Table 1, and data are generated for the lookup table. Figure 6 shows a sampling of the data collected for the 0 wind, 25 m/s airspeed flight, for $\Delta\chi$ values 60°, 90°, and 120° turns. The arrows indicate the proximity distances recorded by the lookup table. Figure 7 shows the complete values of d_p collected for the zero wind turn at an airspeed of 25 m/s.

VI. Simulation and Results

Note that y_s is the aircraft's cross-track error, i.e. the distance from its commanded flight path. In pure waypoint flying, $y_0 = 0$, but with a look-ahead distance (either fixed or dynamically calculated as d_p), $y_0 \neq 0$; the aircraft begins its course correction some distance from the new course. In these instances the magnitude of y_0 is calculated by constructing an orthogonal projector from the aircraft's current position $\mathbf{P}$

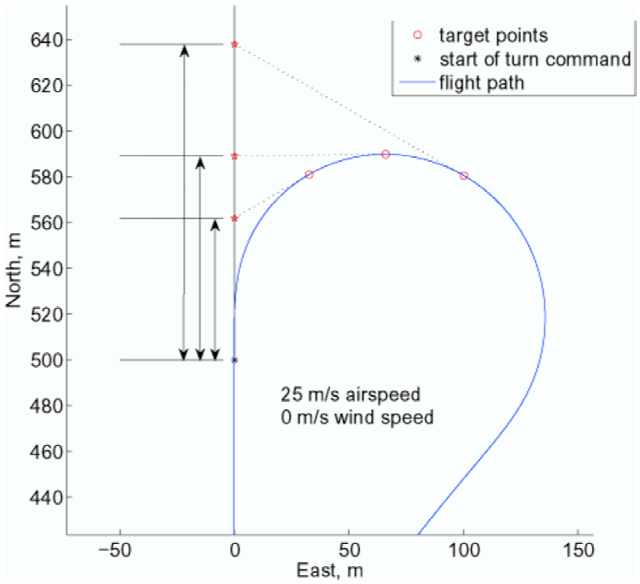

Figure 6. The flight path for generation of lookup table data — zero wind — 25 m/s commanded airspeed — sample data collection.

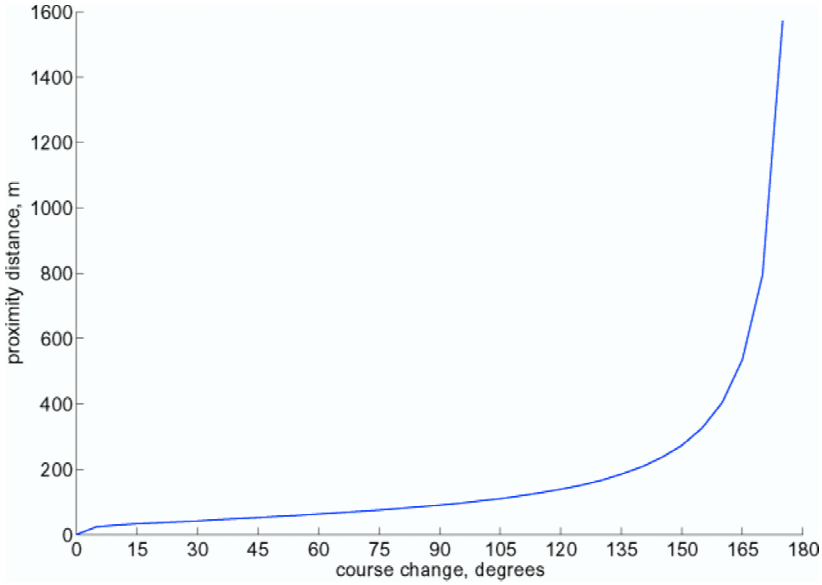

Figure 7. The complete proximity distance values for zero overshoot with 25 m/s airspeed and no wind.

onto the new course[11]

$$|y_0| = [\chi_n(\chi_n^T\chi_n)^{-1}\chi_n^T](\mathbf{W_c} - \mathbf{P}) - (\mathbf{W_c} - \mathbf{P}) \tag{16}$$

The proper sign of y_0 is determined by $\Delta\chi$

$$y_0 = \begin{array}{ll} |y_0| & \text{if } \Delta\chi \leq 0, \\ -|y_0| & \text{otherwise} \end{array} \tag{17}$$

where $\Delta\chi$ is defined from $-180°$ to $180°$. At each time step in the simulation, the lookup table is used to calculate the proper proximity distance. Linear interpolation is used when the input values are between breakpoints. Once the aircraft is within the proximity distance, $||\mathbf{W_c} - \mathbf{P}|| \leq \mathbf{d_p}$, it begins correcting its course and flying to the next waypoint. Adjusting d_p at every time step provides the fastest response to

a shift in wind, but is also the most a 'computationally wasteful' choice. An alternative is to employ the lookup table only after the aircraft has crossed some predetermined threshold, for example within 250 meters of a waypoint.

Figure 8 shows the ground track for a series of landing patterns. Figure 8 (a) is 'pure waypoint' flying without wind; only when the aircraft reaches a waypoint does it look to the next waypoint. For a 90° turn, there is significant overshoot, even without wind. Figure 8 (b) is waypoint flying with a fixed look-ahead distance. In this case, the distance was specifically chosen to correspond to a 90° turn in zero wind, so the ground track shows good convergence without overshoot. In Figure 8 (c) a 10 m/s West wind is added. The fixed look-ahead distance is now insufficient for the turns, resulting in overshoot. Figure 8 (d) shows the same wind conditions flown with the lookup table choosing the proximity distances. In this case, the proximity distances are automatically enlarged to accommodate the larger turn areas necessitated by the wind, thus resulting in a ground track without overshoots.

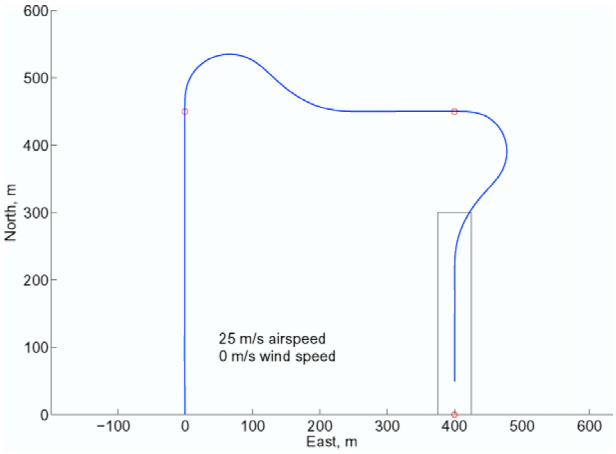

(a) Pure waypoint flying — 0 wind.

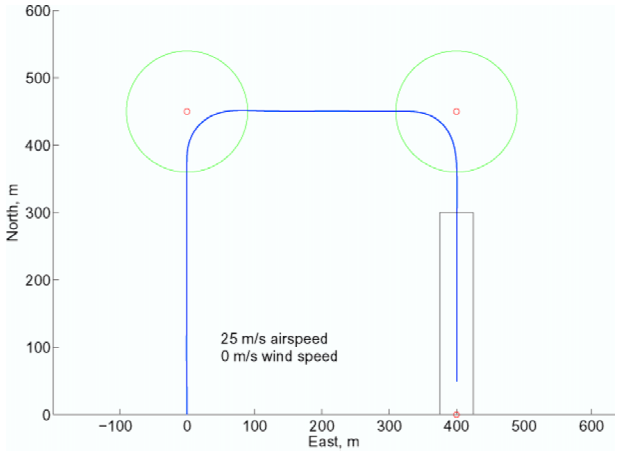

(b) Fixed look-ahead distance — 0 wind.

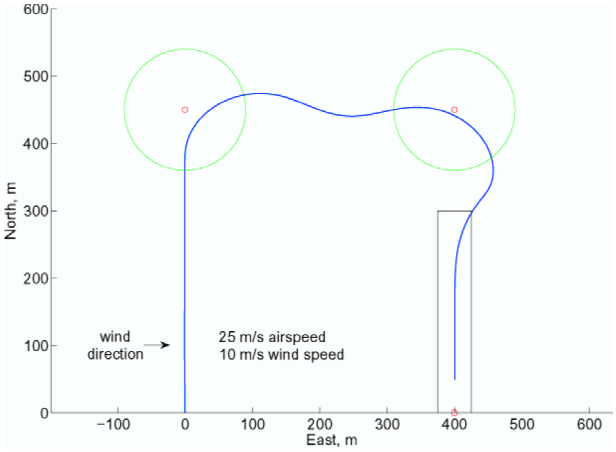

(c) Fixed look-ahead distance — 10 m/s wind from 270°.

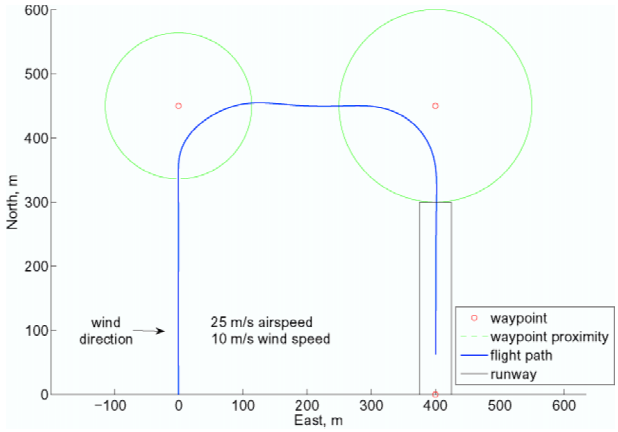

(d) Variable proximity distance — 10 m/s wind from 270°.

Figure 8. A series of simulated landing patterns in different wind environments using different proximity distances.

Figure 9 shows a simple holding or loitering pattern that can be flown while the aircraft awaits further instructions. The concentric waypoint proximity circles in the Southwest corner of the pattern show that two different proximity distances were used, based on the differing $\Delta\chi$ values and relative wind headings.

Finally, Figure 10 shows the aircraft 'circling' a target. The circle is actually a many-sided polygon built with a series of waypoints. The waypoints are automatically generated based on a target position and a desired radius. Flying in wind has no effect on the flight path, since the waypoints are still defined in the shape of a circle. However, in the presence of wind, the ground speed of the aircraft around the circle is no longer uniform. The navigation module will reveal the limiting turn segments from the same table lookup

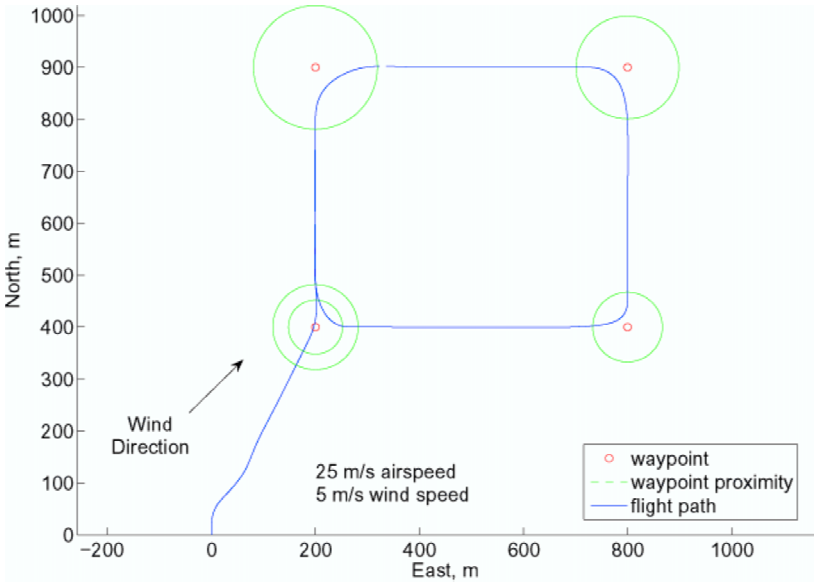

Figure 9. A sample holding pattern flight path. Wind is 5 m/s from 225°.

information (the latter is not demonstrated here, but will be added in the finalized version of this report).

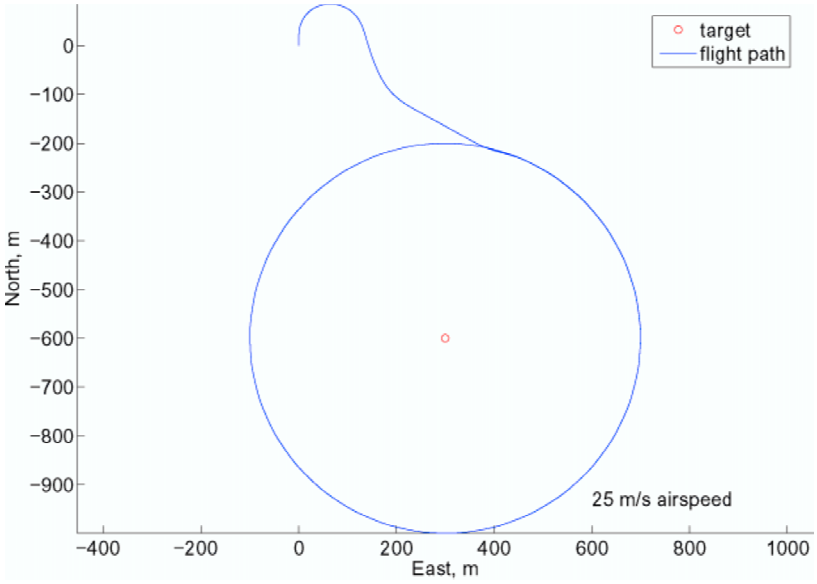

Figure 10. Circling a target in 0 wind — 25 m/s airspeed.

VII. Wind Estimation

The simulation results in this work are based on 'perfect' wind information, i.e. generated wind speed and heading are fed directly into the lookup table. The path-following algorithm is robust enough to allow approximate solutions, relying on a wind speed and direction estimator,[7] which is described next.

The airspeed V_a is measured with airdata instruments, the ground speed V_g and course χ are measured by GPS, and wind speed V_w and direction χ_w are related to the aircraft heading, ψ e.g. in North and East

directions as

$$\begin{aligned} V_g c_\chi &= V_a c_\psi - V_w c_{\chi_w} \triangleq V_a c_\psi + u_w \\ V_g s_\chi &= V_a s_\psi - V_w s_{\chi_w} \triangleq V_a s_\psi + v_w \end{aligned}$$

If wind speed and direction are considered constant (slowly varying), then these can be considered as 'unknown initial conditions' and obtained by means of an observer. Assuming that the aircraft heading is measured, a nonlinear observer may be constructed to estimate the wind direction and speed. A similar approach to that of Ref.[12] is used.

$$\frac{d}{dt}\hat{\mathbf{x}} = A_o\,\hat{\mathbf{x}} + B_o\,\mathbf{u_o} \tag{18}$$

where

$$\hat{\mathbf{x}}^T = \left(\hat{x}, \hat{y}, \hat{u}_w, \hat{v}_w \right), \quad \mathbf{u_o^T} = \left(x_N, y_E, V_a c_\psi, V_a s_\psi \right) \tag{19}$$

and

$$A_o = \begin{pmatrix} -\lambda_1 & 0 & 1 & 0 \\ 0 & -\lambda_2 & 0 & 1 \\ -\lambda_3 & 0 & 0 & 0 \\ 0 & -\lambda_4 & 0 & 0 \end{pmatrix}, \quad B_o = \begin{pmatrix} \lambda_1 & 0 & 1 & 0 \\ 0 & \lambda_2 & 0 & 1 \\ \lambda_3 & 0 & 0 & 0 \\ 0 & \lambda_4 & 0 & 0 \end{pmatrix} \tag{20}$$

This results in a linear error model as

$$\begin{aligned} \dot{\tilde{x}} &= -\lambda_1 \tilde{x} + \tilde{u}_w \\ \dot{\tilde{y}} &= -\lambda_2 \tilde{y} + \tilde{v}_w \\ \dot{\tilde{u}}_w &= -\lambda_3 \tilde{x} \\ \dot{\tilde{v}}_w &= -\lambda_4 \tilde{y} \end{aligned}$$

where $\tilde{x} \triangleq x - \hat{x}$, et-c. Some results are shown in Figures(11) and (12).

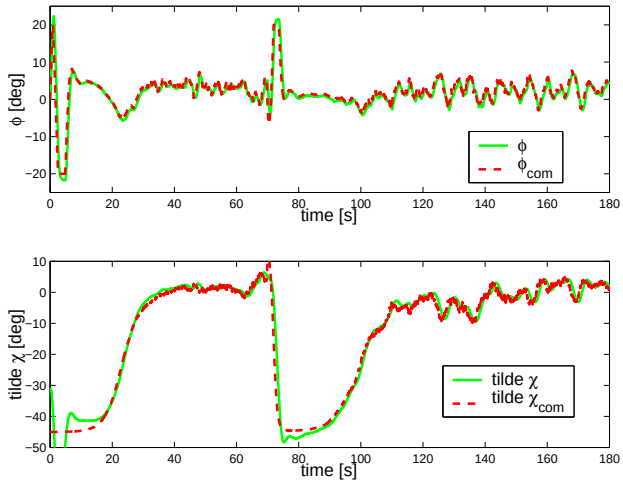

Figure 11. Wind observation: Bank angle and relative course time histories corresponding to figure (12). Besides exposure to a slowly changing wind field, in this example the aircraft is also exposed to Dryden moderate turbulence and an aggressive bank angle control law.

VIII. Future Work

Currently, the lookup table approach produces 'good' results. The aircraft makes smooth transitions between waypoints, and does so without overshoot in most conditions. For course changes that are significantly large than 90^o, avoiding overshoot would require undesirably large turn radii. This can be avoided by applying a cutoff to d_p. For example, d_p values above 200 meters are held constant. Certain turns, like the

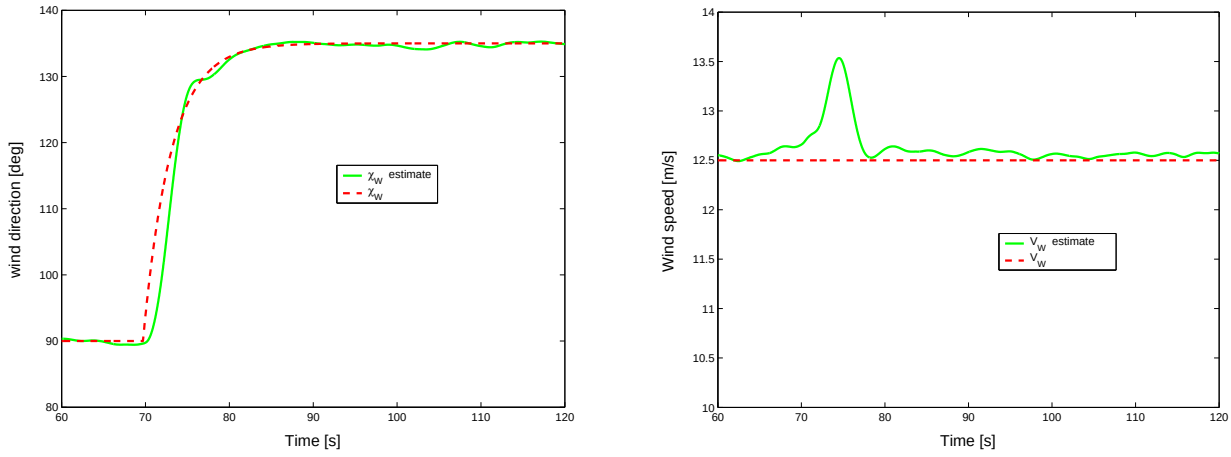

(a) (b)

Figure 12. Wind observation: Trace of the 3 min flight of figure (11) at an airspeed of $V_a = 25\ m/s$, with wind 090^o at $12.5\ m/s$. The aircraft is exposed to a southerly wind-shift of 45^o occurring over $10\ s$. The new wind direction and speed is observed and can subsequently be used as input to the lookup table.

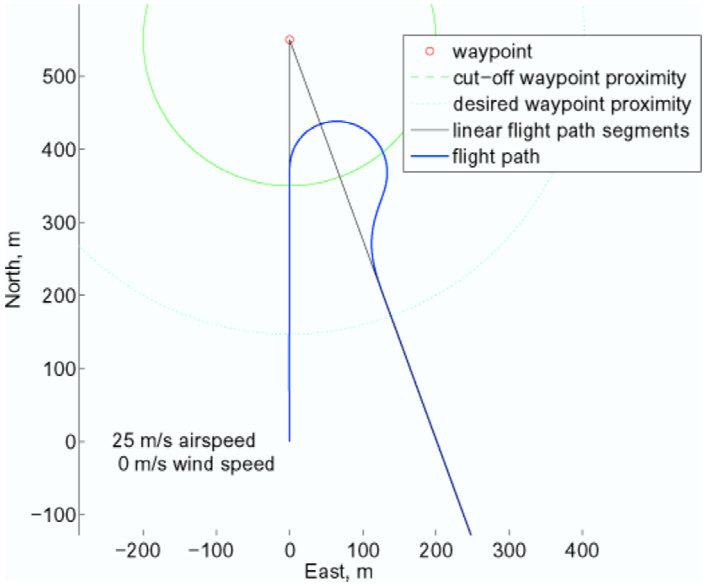

Figure 13. Large angle turn resulting in overshoot of the desired flight segment.

one illustrated in Figure 13, are thus made with some overshoot, a condition that is preferable to 'missing' the waypoint by an otherwise large distance. As a possible remedy, one could define the 'best' turn as minimizing the cumulative distance from the desired path. There are a variety of situations, particularly in strong wind conditions, when the 'good' turn is far from this 'best' turn. For example, an aircraft traveling due North, when commanded to make a 170° turn, will always turn to the right. However, if the wind is from the West, the 'best' turn as defined above would be some overshoot of the target waypoint, followed by a turn into the wind, despite the fact that it results in a turn of 190°. Improved logic for an enlarged lookup table (to handle turns > 180°) should allow for better turns, if not the actual 'best' turn.

Although this paper deals solely with the flight performance of a single UAV, the lookup table approach will be useful with multiple UAVs operating in close proximity in the presence of wind. Close proximity flying is hindered because the turn duration is not controlled, but an extra variable can be added to the lookup table to measure this. With this knowledge, a planner can account for the different turn times and distances. This may benefit flight coordination or formation flying.

IX. Conclusions

The use of a lookup table to alter the look-ahead distance of a UAV is shown to be a viable and efficient method for generating good turns in a variety of wind conditions. It produces results that are superior to either pure waypoint flying or relying on a fixed look-ahead distance. The use of the lookup table in the simulation does not add noticeably to the run-time. Additionally, if the lookup table is based solely on kinematics it can be used regardless of the aircraft type, provided that its flight parameters are within the range of the lookup table and its dynamics and delays are not excessive.

References

[1]Breck W. Henderson. Boeing pilotless condor. *Aviation Week & Space Technology*, 132(16):36, April 23 1990.

[2]P. R. Chandler, S. Rasmussen, and M. Pachter. UAV cooperative path planning. In *Proc. of AIAA Guidance, Navigation and Control Conference*, Denver, CO, 2000.

[3]Yoshiaki Kuwata and Jonathan P. How. Stable trajectory design for highly constrained environments using receding horizon control. In *Proceeding of the 2004 American Control Conference*, Boston, MA, 2004.

[4]Ruggero Frezza. Path following for air vehicles in coordinated flight. In *Proceedings of the 1999 IEEE ASME*, pages 884–889, Atlanta, GA, September 19-23.

[5]Anawat Pongppunwattana and Rolf Rysdyk. Real-time planning for multiple autonomous vehicles in dynamic uncertain environments. *AIAA JACIC*, pages 580–604, December 2004.

[6]Dynamic model of aerosonde uav. web-site. Unmanned Dynamics LLC., http://www.u-dynamics.com/aerosim/.

[7]Rolf Rysdyk. UAV path following for constant line-of-sight. In 2^{nd} *AIAA "Unmanned Unlimited" Conf. and Workshop and Exhibit*, San Diego, CA, 2003.

[8]B.Etkin. *Dynamics of Atmospheric Flight*. John Wiley & Sons, New York, 1972.

[9]Morten Breivik and Thor I. Fossen. Principles of guidance-based path following in 2d and 3d. In *44th IEEE Conference on Decision and Control*, Seville, Spain., December 2005.

[10]Isaac Kaminer, Antonio Pascoal, Eric Hallberg, and Carlos Silvestre. Trajectory tracking for autonomous vehicles: An integrated approach to guidance and control. *Journal of Guidance, Control, and Dynamics*, 21(1):29–38, 1998.

[11]Lloyd N. Trefethen and David Bau III. *Numerical Linear Algebra*. SIAM, Philadelphia, 1997.

[12]Encarnaçao, Pascoal, and Arcak. Path following for autonomous marine craft. In *5th IFAC Conference on Marine Craft Maneuvering and Control*, pages 117–122, Aalborg, Denmark, August 2000.